Transparent Fluoride Glass-Ceramics with Phase-Selective Crystallization for Middle IR Photonics

Longfei Zhang[a,b,†] Yang Sun[c,d,†] Yiguang Jiang*[a] Bo Da[e] Juan Du[a,f] Shuaipeng Wang[a] Sisheng Qi[a] Zhiyong Yang[a] Long Zhang[*a,f] and Jin He[*a,f]

[a.] Key Laboratory of Materials for High Power Lasers and State Key Laboratory of High Field Laser Physics, Shanghai Institute of Optics and Fine Mechanics, Chinese Academy of Sciences, Shanghai 201800, China

[b.]Center of Materials Science and Optoelectronics Engineering, University of Chinese Academy of Sciences, Beijing 100049, China

[c.] Department of Applied Physics and Applied Mathematics, Columbia University, New York, NY 10027, USA

[d.] Department of Physics, Iowa State University, Ames, IA 50011, USA

[e.] Research and Services Division of Materials Data and Integrated System, National Institute for Materials Science, 1-1 Namiki, Tsukuba, Ibaraki 305-0044, Japan

[f.] Hangzhou Institute for Advanced Study, UCAS, Hangzhou, Zhejiang 310024, China

[†]Longfei Zhang and Yang Sun contributed equally to this work.

1. Design Principles for Selective Phase-separation Engineering

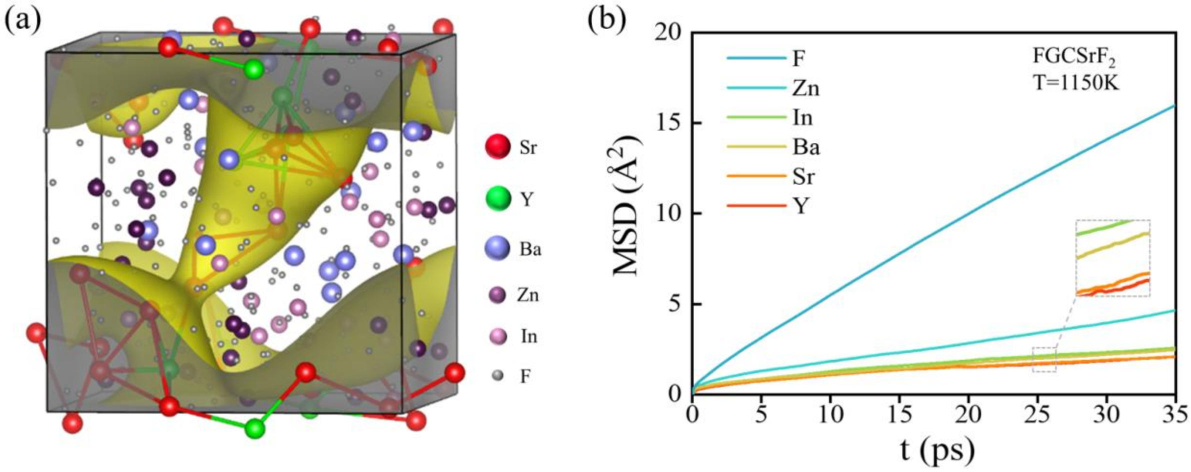

Figure S1 (a) Atomic isosurface from AIMD simulation of $FGCSrF_2$ at T=1150K; (b) Atomic diffusion coefficient in the $FGCSrF_2$ melt at 1150K.

2. Crystallization kinetics and thermodynamic parameters of FGCs

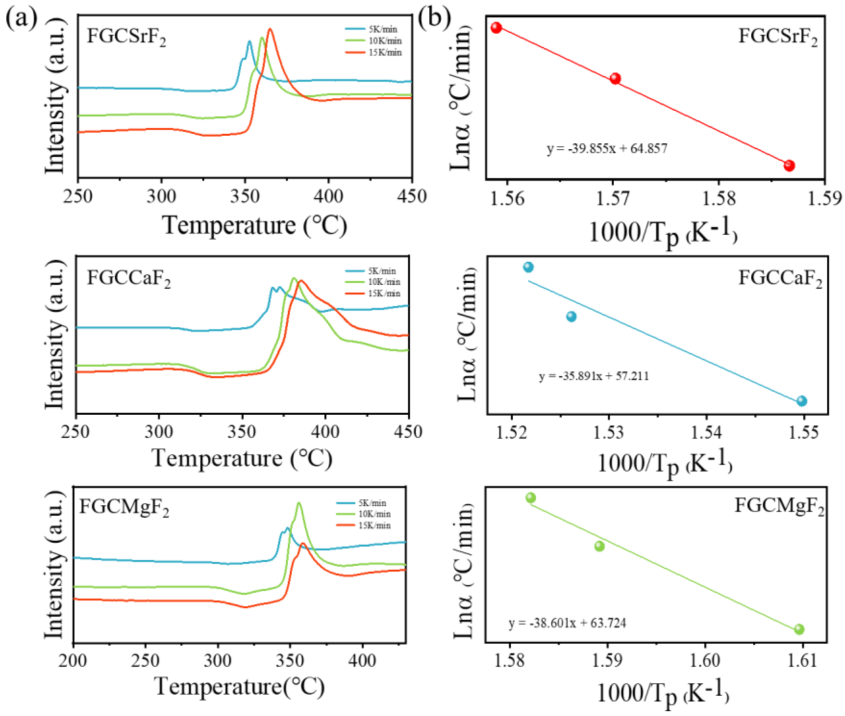

Figure S2 (a) DTA curves under heating rate at 5K/min, 10K/min, and 15K/min for FGCs; (b) the relationship of $Ln\alpha$ between $1/T_p$.

The calculation of crystallization activation energy is based on Owaza equation and evolved from AMT equation:

$$Ln\alpha = -E/RT_p + C$$

where α is the heating rate of DTA analysis. T_p is the exothermic peak temperature of crystallization, which can read from Fig.S2a. C is a constant. R is the gas constant, which equals 8.31441 J/mol·K. Accordingly, the slope (-E/R) of the curve can be obtained by plotting according to the equation, as shown in Fig.S2b. Therefore, the crystallization activation energy (E_c) can be calculated, and the values are presented in **Table S1**.

Table S1 The crystallization activation energy (E_c) of FGCs.

	-E/R	R(J/mol·K)	E(KJ/mol)
FGCSrF_2	-39.855	8.31441	332
FGCCaF_2	-38.601	8.31441	330
FGCMgF_2	-35.891	8.31441	310.3

3. Mechanical properties and corrosion resistance of FGCs

Table S2 Corrosion resistance and Vickers hardness of FGCs and FGInF_3.

	Corrosion resistance test			Vickers hardness (HV)
	Before(g)	After(g)	△W(%)	
FGInF_3	0.4886	0.4840	0.94%	262
FGCSrF_2	0.3143	0.3132	0.06%	273
FGCCaF_2	0.6784	0.6770	0.21%	314
FGCMgF_2	0.7809	0.7752	0.73%	290

4. Refractive index matching degree of two phases in FGCs

Table S3 Refractive index of single crystal (SrF_2, CaF_2, MgF_2) and glass matrix at different wavebands(nm).

	750	1000	2000	3000	5000
SrF_2	1.435	1.433	1.429	1.425	1.412
CaF_2	1.431	1.429	1.424	1.418	1.400
MgF_2	1.375	1.373	1.368	1.360	1.340
Glass	1.487	1.485	1.482	1.480	1.479

(Refractive index data of single crystal and glass matrix are only approximate values, because the refractive index changed as the entrance of other cations in the crystal phase.)

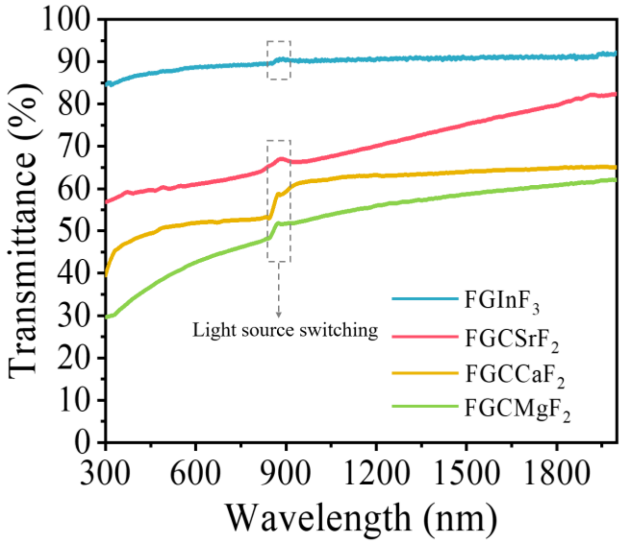

Figure S3 Transmittance in the range of 300 to 2000 nm of FGCs and fluoroindate glass.

5. Control experiment of phase-selective crystallization

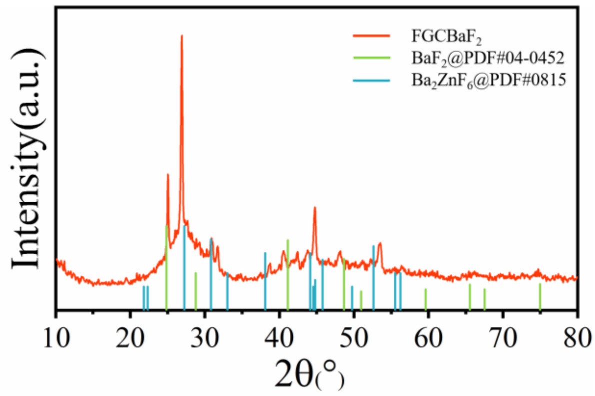

Figure S4. XRD patterns of $FGCBaF_2$, PDF#04-0452 of BaF_2 crystal, and PDF#21-0815 of Ba_2ZnF_6 crystal.

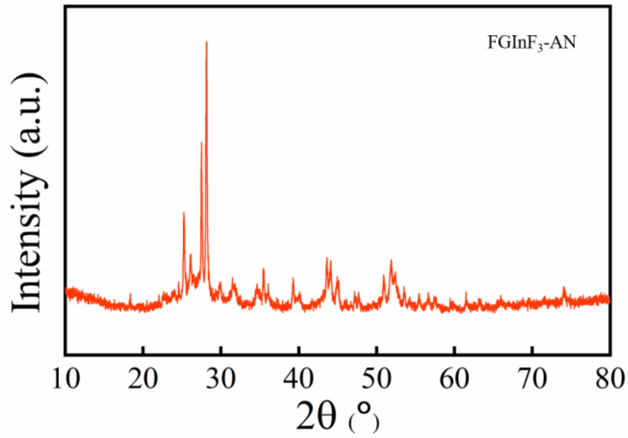

Figure S5 XRD pattern of $FGInF_3$ after classical quenching-annealing-crystallization route.

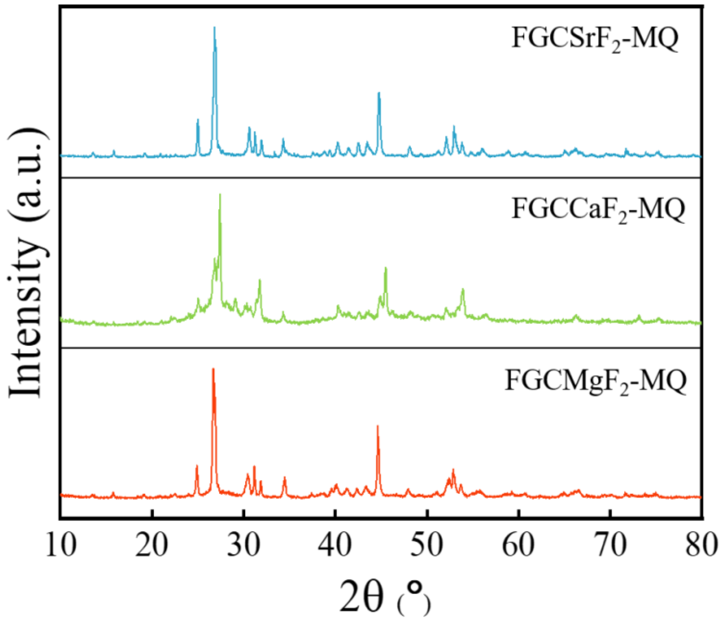

Figure S6 XRD patterns of FGCs samples obtained by traditional one-side melt-quenching.

6. The structure of the FGCs

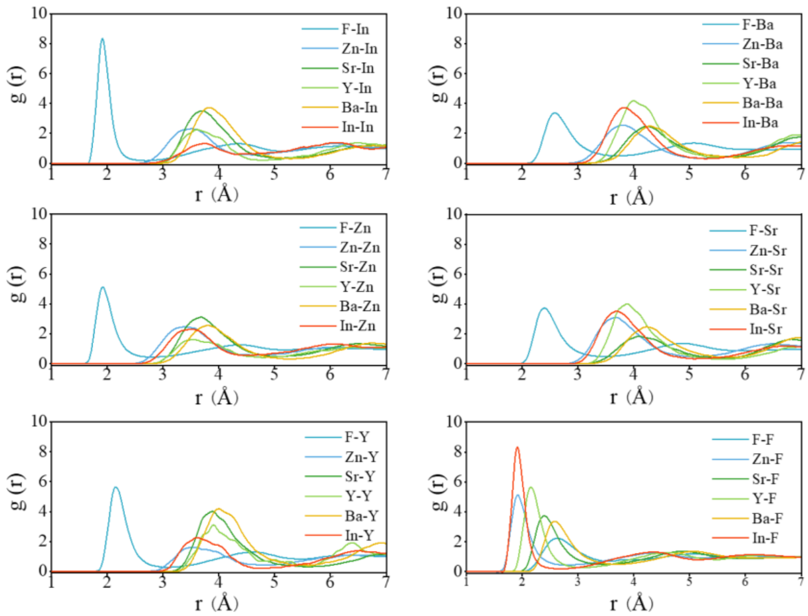

Figure S7 Pair correlation function at 1150K of $FGCSrF_2$.

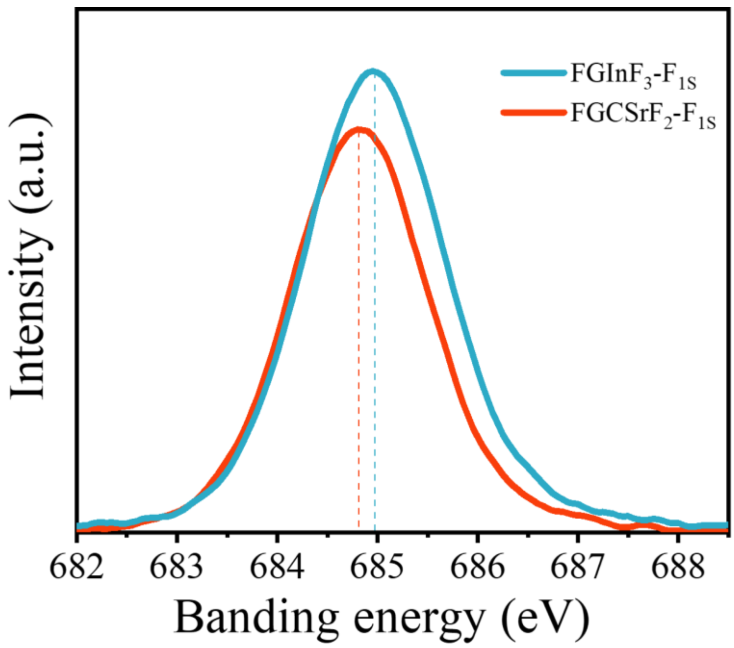

Figure S8 F-1s XPS peak profiles of $FGCSrF_2$ and $FGInF_3$.

7. The UC lifetimes of the FGCs and $FGInF_3$

Analysis of the upconversion luminescence transient for the $^4S_{3/2} \rightarrow {}^4I_{15/2}$ was performed using a best-fit analysis that employed the relationship[1]:

$$I_t = I_0 + A_1 \exp(-t/\tau_1) + A_2 \exp(-t/\tau_2) + A_3 \exp(-t/\tau_3) \quad (1)$$

Where A is fitting parameters, τ is the decay constant. The fitting results are presented in **Figure S4**. The average lifetimes τ are obtained by:

$$\tau = \frac{A_1\tau_1^2 + A_2\tau_2^2 + A_3\tau_3^2}{A_1\tau_1 + A_2\tau_2 + A_3\tau_3} \quad (2)$$

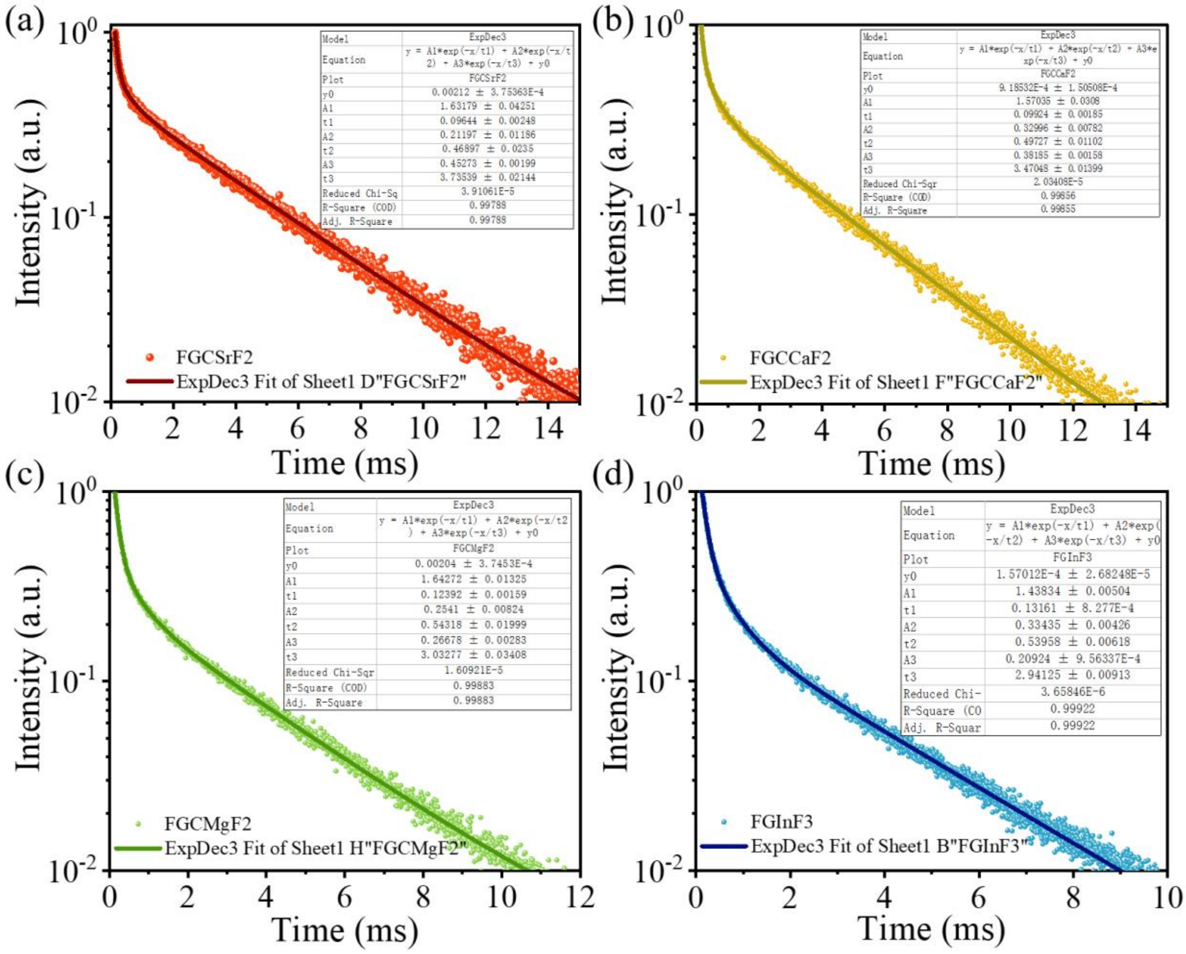

Figure S9 The decay curves of Er^{3+}: $^4S_{3/2}$ of the (a)$FGCSrF_2$, (b)$FGCCaF_2$, (c)$FGCMgF_2$, and (d)$FGInF_3$.

Table S4 Lifetime-related data of FGCs and FGInF3.

	A_1	t_1(ms)	A_2	t_2(ms)	A_3	t_3(ms)	**τ (ms)**
$FGCSrF_2$	1.6318	0.0964	0.2120	0.4690	0.4527	3.7354	**3.27471**
$FGCCaF_2$	1.5704	0.0992	0.3300	0.4973	0.3819	3.4705	**2.85459**
$FGCMgF_2$	1.6427	0.1239	0.254	0.5432	0.2668	3.0328	**2.21954**
$FGInF_3$	1.4383	0.1316	0.3344	0.5396	0.2092	2.9413	**1.96154**

Reference:

1. L. Gomes, V. Fortin, M. Bernier, F. Maes, R. Vallée, S. Poulain, M. Poulain and S. D. Jackson, *Opt. Mater.*, 2017, **66**, 519-526.